Autonomous and Precise Navigation of the PROBA-2 Spacecraft

Oliver Montenbruck[*] and Markus Markgraf[†]
Deutsches Zentrum für Luft- und Raumfahrt (DLR), German Space Operations Center (GSOC), D-82234 Wessling, Germany

Joris Naudet[‡]
Verhaert Space NV, Hogenakkerhoekstraat 9, 9150 Kruibeke, Belgium

and

Stefano Santandrea[§], Kristof Gantois, and Pierrik Vuilleumier
ESA/ESTEC, Keplerlaan 1, 2201 AZ Noordwijk, The Netherland

PROBA-2 is the second technology demonstration mission within the project for onboard autonomy of the European Space Agency (ESA). Besides other instruments and sensors, the micro-satellite will be equipped with two new types of global positioning system (GPS) receivers. These will support the spacecraft operations and demonstrate recent advances in the field of autonomous real-time navigation and offline orbit determination for micro-satellites. The paper provides an overview of the key PROBA-2 navigation elements and discusses their scope and capabilities. Special attention is given to the Phoenix-XNS miniature GPS receiver and its embedded navigation function which are presented along with a discussion of the employed filtering and processing algorithms. The impact of PROBA-2 attitude changes on the GPS tracking is analyzed and the employed strategies for minimizing possible outages are presented. Hardware-in-the loop simulations in a signal simulator testbed are used to demonstrate the feasibility of 1 m level real-time navigation using a single-frequency GPS receiver and to demonstrate the overall robustness of the PROBA-2 onboard navigation.

I. The PROBA-2 Mission and Spacecraft

The PRoject for OnBoard Autonomy (PROBA) spacecraft of the European Space Agency (ESA) provides micro-satellite platforms for spaceflight technology demonstration and dedicated science investigations[1]. Following the success of PROBA-1, a next mission is currently under preparation for launch in early 2009. Other than its predecessor, which provides high-quality hyperspectral images of the Earth, the PROBA-2 spacecraft will be devoted to solar observations and measurements of the space environment[2]. Its primary instrument, the "Sun Watcher using APS detectors and image Processing" (SWAP) will obtain images of the solar atmosphere in ultraviolet light at high data rates. In total, PROBA-2 carries four scientific instruments for solar observation and space environment monitoring:

- the Thermal Plasma Measurement Unit (TPMU),
- the Dual Segmented Langmuir Probe (DSLP),
- the Sun Watcher using APS detectors and image Processing (SWAP), and
- the LYman alpha RAdiometer (LYRA).

These instruments will provide early warnings of solar eruptions, and constitute a major contribution to ESA's Space Weather project.

[*] Head GNSS Technology and Navigation Group
[†] GNSS Systems Engineer, Member AIAA
[‡] PROBA-2 AOCS Engineer
[§] PROBA-2 Systems Engineer

Aside from its scientific goals, the PROBA-2 mission provides the opportunity to validate a series of novel spacecraft technology components that have been contributed by the ESA member states:

- the Beppi Colombo Star Tracker of Galileo Avionica (Italy),
- a Micro Digital Sun Sensor (μDSS) of TNO (The Netherlands),
- a dual-frequency Topstar 3000G2 Global Positioning System Receiver of Thales Alenia Space (France),
- a Solid Propellant Cool Gas Generator (SPCGG) of Bradford-Engineering and TNO (The Netherlands)
- a propulsion subsystem of SSTL (United Kingdom)
- a Solar Array concentrator experiment of CSL (Belgium)
- a Science Grade Vector Magnetometer (SGVM) of DTU (Denmark)
- a Li-Ion battery of SAFT (France)
- the Advanced Data Processing and Management System (ADPMS) of Verhaert (Belgium)
- and reaction wheels of Dynacon (Canada).

PROBA-2 is built by Verhaert, Belgium, under ESA contract. The spacecraft has a mass of roughly 120 kg and a size of 60 x 70 x 85 cm (Fig. 1). Electrical power for the operation of the spacecraft bus and payload is provided by two deployable solar panels.

PROBA-2 will be launched as a co-passenger of ESA's SMOS satellite onboard a Eurockot from the Plesetsk cosmodrome and brought into a Sun-synchronous orbit of 728 km altitude using the re-ignitable Breeze upper stage. For the adopted dusk-dawn orbit the angle between the Sun and the orbital plane (beta angle) is always larger than about 60° and eclipses (of at most 17 min) are confined to a few months during the winter season. No eclipses are encountered for about 80% of the year which provides favorable power conditions and offers long periods of continued Sun observations.

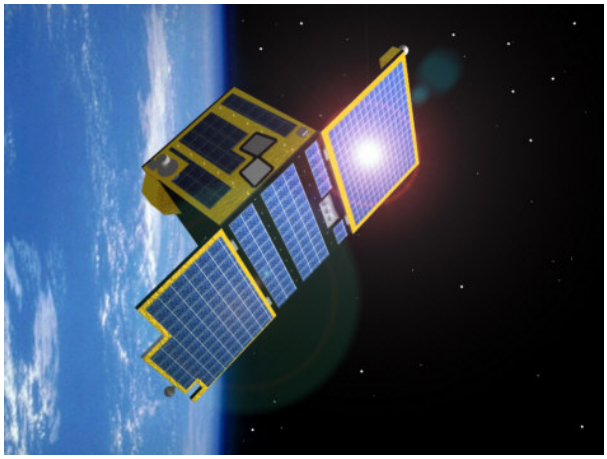

Figure 1. PROBA-2 (artists impression,© ESA)

The PROBA-2 spacecraft employs a redundant Attitude Control and Navigation System (ACNS) based on magnetometer and star sensor measurements as well as magnetorquers and reaction wheels. Besides a safe mode (Bdot mode), the ACNS provides various other control modes supporting different forms of inertial, orbital or target pointing[2]. In the Sun Mode, which constitutes the primary observation mode the –x-axis of the spacecraft will be oriented towards the Sun to enable observations with the LYRA and SWAP instruments. In order to maintain the orientation of the Sun image in the instrument frame, the PROBA-2 spacecraft should ideally maintain a fixed attitude throughout the orbit, whereas the star trackers and GPS antennas must always be pointing away from the Earth. As a compromise four rotations of 90° each are conducted at discrete points in the orbit, thus avoiding star sensor obstructions with minimum impact on the science data collection.

II. PROBA-2 Navigation Architecture

The PROBA-2 spacecraft comprises various navigation related hard- and software components, which are illustrated in Fig. 2.

A cold redundant pair of *Phoenix GPS receivers* contributed by the German Aerospace Center (DLR) constitutes the basic sensor for navigation and timing information with regard to onboard usage and ground based mission support. It provides kinematic position fixes with a representative accuracy of 10 m (3D rms) during normal operations and a pulse per second signal for time synchronization. Raw pseudorange and carrier phase measurements are, furthermore, output on demand to support the performance characterization and precise orbit reconstruction on the ground. The Phoenix receiver board is integrated into the "AOCS interface box" which provides the power conditioning, latch-up protection and line drivers. From here, it connects to the onboard computer in the ADPMS for further processing. A detailed description of the receiver is provided in Sect. III. and its navigation performance is further characterized in Sect. V. In view of limited space for GPS antenna accommodation on the up-looking +z panel of the PROBA-2 spacecraft, the primary and backup GPS receiver are operated from a common antenna via a power divider. However, each receiver employs an independent low noise amplifier (LNA), which is powered from the respective receiver via the radio frequency cable. While the Phoenix

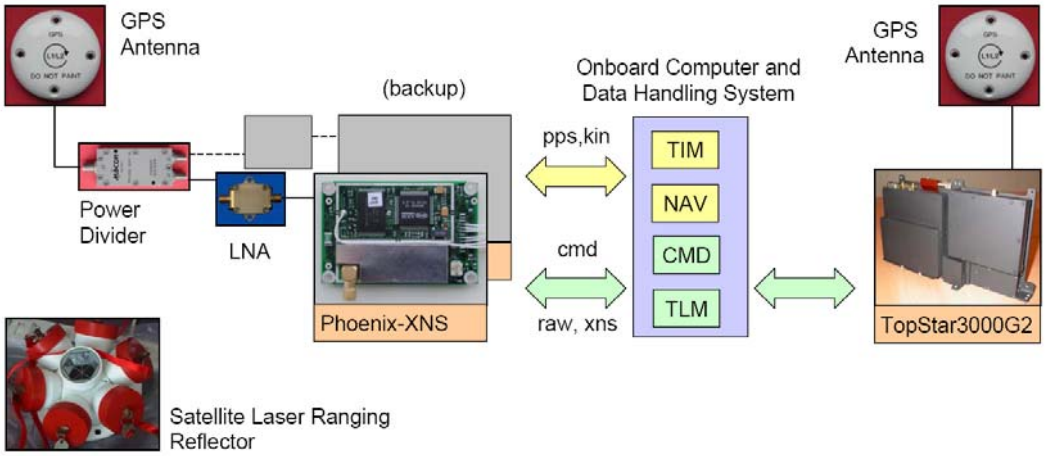

Figure 2. Navigation related system elements of the PROBA-2 spacecraft. See text for further explanations. (T3000G2 image © Thales Alenia Space).

GPS receiver supports only single-frequency tracking, an L1/L2 antenna (Sensor Systems S67-1575-141) is in fact employed for communality with the dual-frequency Topstar3000G2 receiver described below.

The *Navigation (NAV) function* is part of the ACNS software designed by NGC Aerospace, Canada. It operates on a 32-bit LEON2-FT RISC processor with up to 100 MIPS, which is part of the Advanced Data Processing and Management System (ADPMS) and serves as the onboard processor for attitude and orbit computations, data handling and payload processing. The navigation function builds up on flight proven autonomous navigation concepts (Kalman filtering of GPS position fixes, twoline elements orbit propagator, event prediction)[3,4] and extends the algorithms and functionality previously available on PROBA-1 by various PROBA-2 specific elements[5,2]. The navigation function processes kinematic navigation solutions of the Phoenix receiver in a Kalman filter using a low complexity numerical orbit propagator[3]. It provides a smoothed real-time orbit information for onboard purposes and can bridge GPS measurements outages through propagation with the dynamical trajectory model. In case of extended data gaps, an autonomous switch to the redundant GPS receiver branch is initiated. During the initial acquisition and for backup purposes, twoline elements are used as an alternative source of (coarse) orbit information. In this way, the PROBA-2 spacecraft can be properly operated even in case of a complete loss of the GPS sensor. Based on the position and velocity information computed within the NAV function, attitude and pointing directions can be transformed between an inertial (star camera) reference frame and the local-horizontal-local-vertical frame. Along with this, the NAV function provides predictions of auxiliary orbit information and events such as shadow times and Earth exclusion zones[5,2]. PROBA-2 mission specifications require a 200 m (2σ) position accuracy on each axis, which is well below the native GPS measurement accuracy and minimizes the complexity of the required filtering algorithms.

The *Time Management function (TIM)* of the ACNS software provides the synchronization of various time counters (GPS, star sensor, etc.) with the global UTC time scale and filters the jitter of the onboard time[6]. It makes use of the pulse-per-second (PPS) signal of the active Phoenix GPS receiver, and processes the associated GPS time tag provided along with the kinematic navigation solution. The latter is issued within about 80 ms after the PSS event and made available to the onboard computer within another 20 ms. The conversion between GPS and UTC time makes use of a commanded value for the GPS-UTC leap seconds and is thus under full control of the ground operator, whenever a new leap second should be introduced in the future.

The *Topstar3000G2 dual frequency GPS receiver* contributed by Alcatel Alenia Space constitutes one of the PROBA-2 technology demonstration payloads[7]. It is the first European spaceborne GPS receiver capable of tracking the civil navigation signals on both the L1 and L2 frequency and will conduct its maiden flight on PROBA-2. The dual-frequency tracking enables a direct elimination of ionospheric path delays and contributes to more accurate kinematic and dynamically filtered navigation solutions. Compared to the encrypted P(Y)-code signals, which require specialized and often proprietary semi-codeless tracking techniques, the new L2C signal[8] can be tracked directly. This enables a more favorable signal-to-noise ratio and reduces the complexity of the correlator and receiver design. L2C signals have first been transmitted in late 2005 and are presently available on a total of 6 Block-IIR-M GPS satellites. Even though the full operational capability (with L2C transmitted by 8 Block-IIR-M satellites and 16 Block-II satellites) is not expected before 2013[9], a sufficient number (8 or up) of L2C capable GPS

satellites should be available after the launch of PROBA-2 to enable a thorough in-flight validation of the T3000G2 receiver. The receiver itself makes use of a newly developed PEGASE2 correlator chip with a total of 12 tracking channels and supports a correlator spacing down to 1/16th of a chip[7]. The tracking and navigation software is executed on a flight proven ERC32 processor. In the dual-frequency configuration considered for PROBA-2, a total of 6 GPS satellites can be tracked simultaneously. Initial tests conducted in a signal simulator test bed have demonstrated a typical pseudorange accuracy of 2.3 m for L1 C/A code tracking and 3.9 m for L2CS tracking[7]. The higher noise on the L2 frequency is due to the fact that only the Civil Long (CL) component of the multiplexed L2CS signal are processed and a corresponding improvement can be expected in the future by correlating also with the Civil Moderate (CM) component. Besides an instantaneous, kinematic navigation solution, a more accurate dynamically filtered navigation solution is computed by the T3000G2 receiver. For a representative PROBA-2 scenario, a real-time navigation accuracy of better than 5 m (3D rms position) and 0.6 cm/s (3D rms velocity) has been reported by the manufacturer[7]. Depending on the actual number of simultaneously tracked GPS satellites with L1 C/A and L2C signals, a post-facto orbit reconstruction of 0.2-0.5 m can be expected based on the T3000G2 receiver measurements.

As a further experiment, the Phoenix GPS receiver on PROBA-2 is equipped with an *eXtended Navigation System (XNS)*, that can be operated in parallel to the kinematic positioning supported by the standard Phoenix receiver software. The XNS software employs a reduced dynamic Kalman filter for real-time navigation, which is described in full detail in Sect. III.B. Based on a high-grade dynamical modeling and the elimination of ionospheric path delays through a smart combination of code and carrier phase measurements, a 1 m level real-time navigation accuracy can be expected.

The GPS based navigation sensors and real-time navigation systems onboard PROBA-2 are complemented by a *retro reflector for satellite laser ranging (SLR),* which enables a fully independent performance characterization. The laser retro reflector (LRR) flown on PROBA-2 has been built by the Russian Scientific Research Institute for Precision Instruments and is likewise employed for the GOCE and Cryosat missions. It is composed of seven individual prisms and supports laser ranging at angles of up to 70° relative to the normal of the mounting surface. For best tracking conditions, the LRR is mounted opposite to the star cameras and GPS antennas on the –z panel of the PROBA-2 spacecraft. SLR tracking by a global network of observatories has been agreed upon by the International Laser Ranging Service (ILRS)[10] for selected measurement campaigns that will be coordinated with the corresponding GPS tracking experiments on PROBA-2. Ranging accuracies of down to 1 cm are presently achieved by high-grade SLR stations and geodetic grade missions but a somewhat degraded measurement and modeling performance is expected for PROBA-2 due to the non-permanent nadir orientation. Likewise the limited SLR station coverage will not enable a generation of fully independent SLR-based PROBA-2 orbit products. Instead, the available satellite laser ranging measurements will be compared with the GPS derived trajectories to assess the accuracy of the respective sensors and orbit determination results at the level of a few centimeters.

III. The Phoenix GPS Receiver and Navigation System

A. Phoenix - A Miniature GPS Receiver for Space Applications

The Phoenix GPS receiver (Fig. 3) is a miniature receiver specifically designed for high dynamics and space applications[11]. It offers single-frequency C/A code and carrier tracking on 12 channels and can be aided with a priori trajectory information to safely acquire GPS signals even at high altitudes and velocities. The receiver is based on SigTech's commercial-off-the-shelf (COTS) MG5001 board but operates a proprietary firmware developed by DLR. The same approach, albeit with a different firmware, has independently been adopted for SSTL's SGR05U receiver[12]. At a power consumption of less than one Watt and a board size of 50 x 70 mm the receiver is among the smallest of its kind and particularly well suited for satellites with limited onboard resources. Besides several cubesat and demonstration missions, the Phoenix GPS receiver has so far been adopted for use on the PROBA-2, PRISMA, Flying Laptop, TET-1, XSat and RSSP microsatellites.

The Zarlink GP4020 baseband processor chip employed in the Phoenix receiver combines a 12 channel correlator, a microcontroller core with 32 bit ARM7TDMI microprocessor and several peripheral functions (real-time clock, watch-dog, 2 UARTS etc.) in a single package. The MG5001 board, furthermore, provides a 512 kByte flash EPROM for storing the receiver software and a 256 kByte RAM memory for run-time code and data. If desired, the RAM can be doubled for large applications extending the standard receiver functionality. Supplementary to the external memory modules, the GP4020 chip provides a fast internal RAM of 32 kByte size. It is battery buffered and can serve as non-volatile memory for critical receiver parameters almanac, broadcast ephemerides and orbit elements of the user spacecraft.

Figure 3. Phoenix GPS receiver board (PROBA-2 engineering model)

Though originally designed for automotive applications, the receiver board has been qualified for space use in a series of thermal-vacuum, vibration and total ionization dose tests. Tests conducted with a Co-60 gamma radiation source[13] demonstrate that the MG5001 receiver board can tolerate a total ionizing dose (TID) of up to 15 krad (Si). This is compatible with previous tests and flight experience for the GP2021 chip-set and is expected to allow operation in low Earth orbit (LEO) for at least several years. Tests conducted by SSTL as part of the SGR-05 qualification program[14] have shown that the GP4020 correlator will experience no latch-ups below about 15 MeVcm^{2}mg^{-1}, and a saturated cross-section above around 10^{-4} cm^2/device. On the other hand, the GP4020 internal RAM was found to be quite sensitive to upsets with a threshold of around 3 MeV cm^{2}mg^{-1} and $1.5 \cdot 10^{-7}$ cm^2/bit cross-sectional area. For latch-up protection, a rapid fuse is incorporated into the Phoenix power supply as part of the AOCS interface box that hosts the receiver on PROBA-2.

Specific features of the Phoenix receiver software for low Earth orbit (LEO) applications include optimized tracking loops for high accuracy code and carrier tracking, precision timing and integer ambiguities for carrier phase based relative navigation, a twoline elements orbit propagator for signal acquisition aiding, and an attitude interface to account for non-zenith pointing antennas in the channel allocation process. A wide-band 3rd order phase-locked loop with FLL assist is employed for carrier tracking and a narrow-band carrier aided delay-lock loop for code tracking. This ensures robust tracking and avoids systematic steady state errors even under high signal dynamics. Representative noise values of 0.5 m, 0.8 mm and 0.1 m/s are obtained for pseudorange, carrier phase and Doppler data, respectively, at average C/N_0 values of 42 dB-Hz (Fig. 4). For use within the kinematic navigation solution, smoothed pseudoranges with a noise level of about 0.1 m and range-rate measurements from time-differenced carrier phases with a noise level of 2 cm/s are, furthermore, available. Double-difference carrier phases exhibit integer ambiguities for use in differential positioning techniques. All measurements are closely synchronized to integer GPS seconds with a representative accuracy of 0.2µs and a 1 pulse-per-second hardware signal is generated at the same instant. If required, intermitted operation of the receiver is supported through orbital elements stored in non-volatile memory, the battery backed real-time clock and the built-in orbit propagator. This allows a warm or hot start with typical times to first fix of 2 min and 30 s, respectively. After a cold start, a first navigation solution is typically obtained within nine minutes and the time-to-first-fix (TTFF) did not exceed 15 min in 92% of all restarts in an extended signal simulator test campaign.

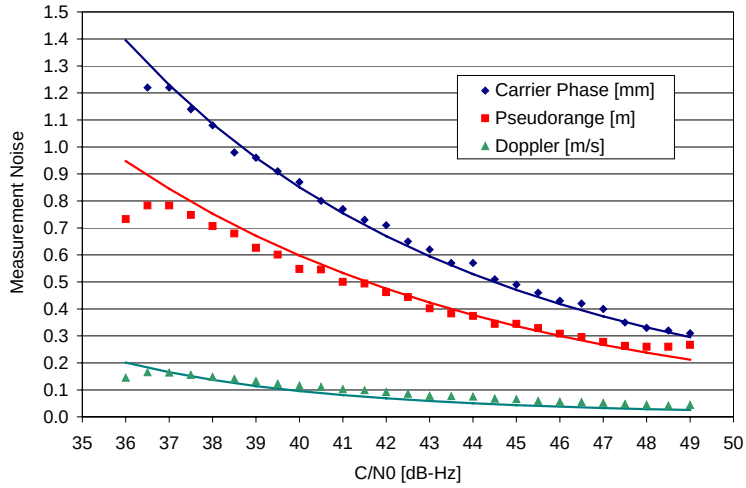

Figure 4. Phoenix measurements noise versus carrier-to-noise-density ratio

To improve the coverage with GPS tracking data in the PROBA-2 mission, the Phoenix receiver software has been upgraded with a PROBA-2 specific satellite selection and channel allocation algorithm. While the +z face of the spacecraft should ideally be oriented in the anti-Earth direction at all times to avoid star sensor obstructions and to ensure an optimum GPS visibility, a continuous roll about the x-axis would be highly undesirable from a payload operations point of view. As a compromise, attitude changes of the PROBA-2 spacecraft are confined to discrete roll-maneuvers about the Sun-pointing axis, which are nominally conducted four times per orbit[2,5]. This maximizes the intervals for continuous Sun observations with the LYRA and SWAP instruments, avoids Earth blinding of the star sensors and ensures a reasonable sky coverage of the GPS antenna field of view. However, the actual antenna boresight might differ by up to 45° from the zenith orientation that is normally assumed by a GPS receiver in the prediction of visible GPS satellites. The new PROBA-2 specific satellite selection and channel allocation mode of the Phoenix receiver accounts for the nominal spacecraft orientation based on a slightly simplified model of the attitude control mode. Depending on the current orbital position one out of four possible orientations (with either, +z, +y, -z, or –y pointing in the direction of the ecliptic north pole) is assumed that minimizes the angle between the local zenith direction and the +z spacecraft axis (Fig. 5). All GPS satellites within a (configurable) 85° cone about the resulting axis are then considered for tracking. While the simplified model in the Phoenix receiver ignores the finite time for execution of the 90° roll maneuvers (labelled as A and B in Fig. 5) it still gives a close match with the real spacecraft orientation and does not require an active interface with the attitude control system.

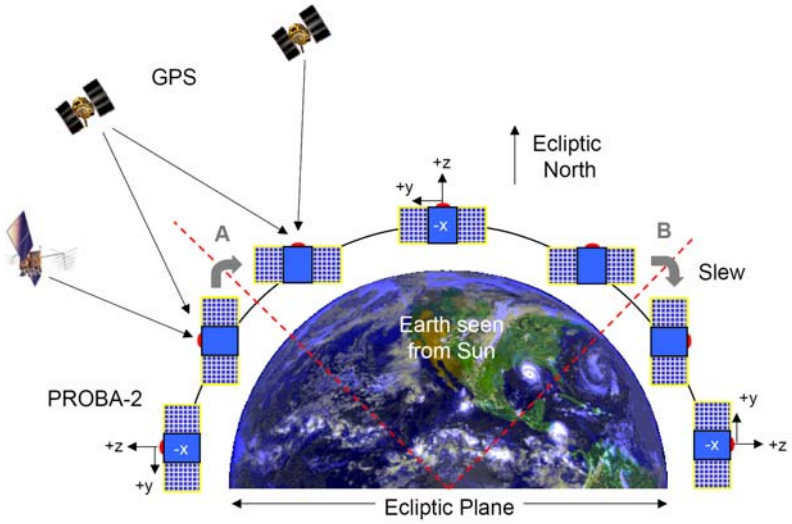

Figure 5. Orbit dependent attitude variation of the PROBA-2 spacecraft

Another extension of the standard Phoenix receiver software is the eXtended Navigation System (XNS)[15] that will for the first time be demonstrated as a flight experiment onboard the PROBA-2 satellite. It offers a dynamically smoothed and continuous navigation solution even in case of limited GPS satellite visibility. The measurement processing inside the Phoenix-XNS provides a rigorous elimination of ionospheric path delays and enables a real-time navigation accuracy meeting the requirements of advanced remote sensing satellites. The XNS employs a ionosphere-free code-carrier combination, which is also known as GRAPHIC (Group and PHase Ionospheric Correction) measurement. Processing of the GRAPHIC data is complicated by the need to handle channel specific biases, which must be estimated along with the spacecraft state, force model parameters and the receiver clock offset. The dynamical trajectory model adopted in the XNS accounts for the aspheric gravitational potential of the Earth, luni-solar gravitational perturbations, solar radiation pressure and atmospheric drag. Remaining imperfections of the dynamical model are compensated by empirical accelerations that are treated as exponentially correlated random variables in the extended Kalman filter.

The XNS is implemented as a low priority task that runs concurrently with the standard signal tracking and positioning software of the Phoenix receiver. It is entirely written in C++ which provides a high level of abstraction and notably simplifies the coding of the dynamical model, Kalman filtering , and measurement modeling. Filter update steps are performed once every 30 s and a polynomial representation of the propagated orbit is used to obtain dense position and velocity information at intermediate epochs. Despite the high modeling complexity and the required execution time for a single update step the XNS is thus compatible with the available spare computing resources (roughly 50%) of the unmodified Phoenix receiver. The proper operation of the Phoenix-XNS navigation system has been demonstrated in a series of signal simulator tests for polar LEO orbits, in which a representative 3D position error of 1 m has been achieved[15]. Except for a memory upgrade (512kB total), the XNS software can be executed on a standard Phoenix (MG5001) receiver board and does not require an external navigation processor.

B. XNS Real-Time Navigation Algorithms

The XNS employs a traditional extended Kalman filter to estimate the orbit of the host spacecraft using raw GPS measurements. Similar systems have earlier been discussed by various authors[16-18] and most of the relevant algorithms are readily described in standard text books[19-21]. The subsequent discussion is therefore focused on specific aspects that are of relevance for a better understanding of the achievable accuracy as well the XNS run-time performance and operations.

At the core of the XNS, a high-fidelity reduced dynamic orbit model is used for the prediction of the spacecraft motion between consecutive Kalman filter update steps. The model accounts for the gravitational attraction of the Earth, Sun, and Moon as well as non-gravitational forces due to atmospheric drag and solar radiation pressure. A recent gravity field model derived from the GRACE mission (GGM01[22]) has been adopted and the resulting acceleration is efficiently computed using the Cunningham recurrence relations[23,20]. In accord with the orbital altitude of PROBA-2, gravity coefficients up to degree and order 40 are considered in the XNS default configuration for this mission. This choice limits the computational effort without sacrificing the achievable accuracy[24], but higher order terms can always be activated by telecommand if desired. Likewise, a provision for the consideration of solid-Earth tides[25] has been made but need not be considered for PROBA-2. For the modeling of luni-solar perturbations a point mass model is employed and the respective body-coordinates are obtained by low-precision analytical series expansions[20]. In case of the Sun, only the elliptic motion relative to the Earth-Moon barycenter is considered, while the lunar motion model takes into account the dominant perturbations (major and annual inequalities, evection, variation, etc.) as well. The series achieve a representative accuracy of 0.02° and 0.1° for the Sun and Moon, respectively, which is sufficient for modeling the perturbing acceleration on a low Earth satellite down to a level of 10 nm/s^2. Drag and solar radiation pressure are described by cannon-ball models[20] with adjustable scaling factors (C_R, C_D) describing the reflective and ballistic properties of the spacecraft. The radiation pressure model takes into account a conic shadow model for the Sun but ignores penumbra effects, Earth albedo, and lunar shadows. For the computation of the atmospheric density a Harris-Priester model[26,20] with static coefficients for mean solar-activity has been adopted in view of its simplicity. While more refined models can, in principle, provide a better description of the actual density, the required environmental parameters (solar flux, mean solar flux, geomagnetic activity index) can hardly be made available in real-time onboard a spacecraft. As such, the better modeling accuracy cannot be properly materialized in an autonomous navigation system. However, modeling deficiencies can, to a fair extent, be absorbed in the adjustment of the ballistic coefficient as well as supplementary empirical accelerations in radial, along-track and cross-track direction within the Kalman filter. The empirical accelerations are treated as exponentially correlated random variables[21] in the filter model and applied as piecewise constant accelerations in the trajectory model when propagating the orbit between epochs. As a rule of thumb, the deterministic part of the XNS force model accounts for accelerations down to roughly 100 nm/s^2, while the estimated empirical accelerations account for the remaining difference between the a priori model and the real world dynamics.

Transformations between the celestial and terrestrial reference frame that occur quite naturally in the modeling of individual force model contributions are based on the IERS1996 conventions[27] and make use of heritage models for precession, nutation, Earth rotation and polar motion[28]. Earth orientation parameters such as the UT1-UTC difference and the pole coordinates are treated as constant parameters in the present XNS implementation and can be updated through telecommands if deemed necessary. The UTC-GPS difference is available from the GPS navigation message and enables an adequate modeling of the Earth rotation in terms of GPS time even if no UT1-UTC correction is available. The position and velocity estimated by the XNS are always expressed in an Earth fixed frame, which is implicitly aligned with the WGS84 system used for the description of GPS broadcast ephemerides. Thus, errors in the knowledge of the Earth orientation parameters affect only the internally computed inertial coordinates but are of limited relevance for the XNS performance.

Besides the fact that a navigation solution in the Earth-fixed reference frame is well suited for a wide range of applications (geocoding, target pointing, etc.), it may also be noted that the modeling of GPS measurements is normally performed in this very frame[8]. Likewise the dominating perturbations (Earth oblateness and asphericity, atmospheric drag) in the trajectory model are most naturally described in a co-rotating, Earth-fixed coordinate system. With this background, a consistent, Earth-fixed formulation for the equation of motion has been adopted in the XNS design. Compared to the common praxis of using a purely inertial formulation, the overall need for reference system transformations and, to a limited extent, the impact of associated modeling simplifications can thus be minimized. On the other hand, a proper account of Coriolis and centrifugal accelerations

$$\Delta \boldsymbol{a} = -2\boldsymbol{\omega} \times \boldsymbol{v} - \boldsymbol{\omega} \times \boldsymbol{\omega} \times \boldsymbol{r} \tag{1}$$

is mandatory, where $\boldsymbol{\omega}$ denotes the instantaneous rotation vector and $\boldsymbol{r}$ and $\boldsymbol{v}$ are the position and velocity in the rotating Earth-fixed reference frame. While the rigorous computation of $\boldsymbol{\omega}$ requires full knowledge of the time derivative of the inertial-to-Earth-fixed transformation, the simplified expression

$$\boldsymbol{\omega} \approx \boldsymbol{\Pi}(t) \cdot \begin{pmatrix} 0 \\ 0 \\ \omega_{\oplus} \end{pmatrix} \tag{2}$$

with a fixed Earth rotation rate $\omega_{\oplus} = 0.7292115 \cdot 10^{-4}\,\text{rad/s}$ and the instantaneous polar motion matrix $\boldsymbol{\Pi}(t)$ can be applied in practice. It takes into account that the rotational axis of the Earth is slightly tilted relative to the adopted polar body axis. Despite the small size of the polar motion angles (<0.5") the consideration of polar motion notably improves the modeling accuracy of the Coriolis and centrifugal forces and ensures consistency with the desired overall accuracy of the dynamical force model[24].

Following the successful example of the BIRD onboard navigation system[4], the numerical integration of the equation of motion is performed by a 4th order Runge-Kutta method (RK4) with Richardson extrapolation[29]. Starting from an initial state vector $\boldsymbol{y}(t) = (\boldsymbol{r}(t)\,\boldsymbol{v}(t))$ at time t, a solution at time $t + H$ is first constructed by taking a single RK4 step of size H, then independently by taking two consecutive steps of size $h = H/2$. The two results are then used to extrapolate the solution that would be obtained for an infinitely small step size. Three individual RK4 steps are thus employed per macro-step H, which implies an average of 5.5 acceleration computations per (micro-)step h. However, the resulting solution is effectively of order 5 and could not be obtained at the same cost with a standard 5th order RK method. Besides its efficiency, the Richardson extrapolation also facilitates the generation of an interpolating polynomial. Making use of the known state vector and its derivatives at times t, $t + H/2$, and $t + H$, a Hermite polynomial can be constructed, which results in a consistent 5th order integrator and interpolant[29,30]. Irrespective of the measurement update rate, XNS solutions at intermediate epochs can thus be obtained from the interpolating polynomial provided at output rates up to a user configurable maximum of 1 Hz.

The state transition matrix of the position-velocity vector and the associated partial derivatives with respect to the force model parameters (drag and radiation pressure coefficients as well as empirical accelerations) are obtained by a rigorous numerical integration of the associated variational equation. However, some simplifications (only low order zonal gravity field, no luni-solar perturbations) are made in this case to avoid an excessive computational load.

The measurements processed in the Phoenix-XNS are a simple linear combination

$$\rho^* = (\rho_{\text{PR}} + \rho_{\text{CP}})/2 \tag{3}$$

of the elementary pseudorange (ρ_{PR}) and carrier phase measurements (ρ_{CP}) on the L1 frequency. This so-called GRAPHIC (Group and Phase Ionospheric Correction) combination introduced by Yunck[31] makes use of the fact that ionospheric path delays (I) affect code and phase measurements in an opposite manner due to the difference of the group and phase velocity in a dispersive medium. Given the geometric range ρ between the GPS satellite and the receiver as well as the corresponding clock offset terms cdt_{GPS} and cdt, the elementary measurements can be described by the relations

$$\begin{aligned} \rho_{\text{PR}} &= \rho + c(\delta t - \delta t_{\text{GPS}}) + I \\ \rho_{\text{CP}} &= \rho + c(\delta t - \delta t_{\text{GPS}}) - I + A\lambda \quad . \end{aligned} \tag{4}$$

Here, $A\lambda$ represents an unknown bias that is a float valued multiple of the wavelength λ and results from the ambiguity of the carrier phase measurement process as well as receiver and transmitter dependent line biases. Evidently the GRAPHIC combination fully eliminates the ionospheric range delay and the combined measurement can be modelled as a biased pseudorange

$$\rho^* = \rho + c(\delta t - \delta t_{\text{GPS}}) + B \tag{5}$$

with $B = A\lambda/2$ denoting a pass-dependent bias that is constant for each arc of continuous carrier phase tracking. Besides being independent of ionospheric path delays, the GRAPHIC combination also exhibits a two times smaller noise level (roughly 0.25 m for the Phoenix receiver) than the pseudorange measurements. However, its processing

is complicated by the need to adjust the GRAPHIC biases along with other state parameters within the real-time navigation filter.

The modeling of the geometric range between the GPS satellite and receiver in the XNS software matches that of the basic kinematic navigation solution. It is based on GPS satellite positions derived from the real-time broadcast ephemeris parameters and takes into account conventional corrections for light time and Earth rotation during the signal propagation (see Refs. 8,32). Similarly, the computation of the GPS receiver clock offset is based on the polynomial clock coefficients provided in the navigation message with corrections of periodic relativistic clock variations. Receiver clock offsets are generally small (<0.1μs) due to the active clock steering of the Phoenix receiver time to GPS time. As such, the measurement time tag can be identified with GPS time and no dedicated clock correction is required prior to processing the measurements in the navigation filter.

The GRAPHIC measurements are processed in an extended Kalman filter which provides estimates of the spacecraft position and velocity at the respective measurement epochs. Along with these, the filter adjusts the drag and radiation pressure coefficients, the three empirical accelerations, a receiver clock offset and one bias parameter for each tracking channel. The estimation state vector thus comprises a total of 24 individual components. Measurement updates are performed once every 30 s using the latest set of measurements available at the invocation of the XNS task. Thereafter, the trajectory is propagated beyond the epoch of the subsequent measurement update (taking into account the expected total processing time) and the corresponding interpolating polynomial is computed. In this way, trajectory information for onboard use at arbitrary sampling rates is continuously available, even though the filter is only operated at a very moderate sampling rate. The time update step makes use of the precomputed, interpolated orbit information for the new measurement epochs. Clock and bias states as well as the drag and radiation pressure coefficient are propagated as constants, while the empirical accelerations are propagated with an exponential damping factor taking into account the user configurable auto-correlation period. Process noise is considered in the clock offset and empirical acceleration parameters, which are described by a random walk model and a 1st order Gauss-Markov process, respectively. Even though the use of process noise in the bias parameters has been found to be of benefit in some cases[24], this feature is not presently employed in the XNS filter design.

IV. PROBA-2 Precise Orbit Determination and Prediction

Mission operations for the PROBA-2 spacecraft will be performed at the ground station in Redu, Belgium. These comprise the mission planning, scheduling, health monitoring, and commanding of the spacecraft and its payloads. All planning tasks as well as the antenna steering can essentially be based on twoline orbital elements with an inherent accuracy of 2-20 km. For the post-facto experiment data analysis, the navigation solution of the ACNS NAV function is furthermore available as part of the telemetry data stream, which provides orbit information at the 10 m level.

Aside from the above mission elements, a dedicated offline orbit determination and prediction process will be implemented to support the generation of SLR predicts for the PROBA-2 spacecraft during dedicated laser tracking campaigns. Here, a batch least-squares estimator and a state-of-the-art dynamical trajectory model will be used to adjust the spacecraft motion using kinematic GPS position fixes as pseudo-observations. This approach offers some performance improvements over the onboard solution and can typically achieve an orbit restitution accuracy at the 2 m level[33]. More importantly, however, the use of a fully dynamical orbit modeling along with the adjustment of a ballistic coefficient ensures that the resulting state vector can be predicted with the required accuracy over a sufficiently long forecast interval. As a rule of thumb, predictions for LEO orbits must be accurate to 10 ms, or, equivalently, 70 m in along-track direction to enable a successful SLR tracking[34]. The actual prediction interval will depend on the solar activity during the PROBA-2 mission, but a maximum of one predict per day is currently envisaged in view of the high altitude of this spacecraft.

For the in-flight performance analysis of the XNS results, precise orbit determination (POD) solutions will be generated by DLR based on raw Phoenix GPS measurements. The GPS High Precision Software Tools (GHOST[35]) used for this purpose employ high-fidelity dynamical and measurement models and are routinely used for POD of the GRACE and TerraSAR-X satellites at the 5 cm level. For the Phoenix data analysis, GRAPHIC measurements will be processed similar to those used by the XNS itself, but the ground processing will benefit from knowledge of the spacecraft attitude for modeling the antenna offset from the center of mass as well as highly accurate GPS orbit and clock products. The expected accuracy of the post-processed orbit solutions is at the level of 0.5 m and might even be improved by taking into account dual-frequency carrier phase measurements from the Topstar3000G2 receiver. The POD results will first be validated against the SLR measurements and can then be used to assess the performance of the various kinematic and filtered onboard navigations solutions of PROBA-2.

V. Hardware-In-The-Loop Validation

To validate the core elements of the PROBA-2 navigation architecture, different levels of hardware-in-the-loop (HIL) tests have been conducted. In a first step, a stand-alone test of the Phoenix GPS receiver in a signal simulator test bed was performed to validate the basic tracking function, the kinematic navigation solution and the XNS performance under the specific conditions of the PROBA-2 mission profile. In a second step, an integrated GPS/ACNS test at system level was used to assess the proper interaction, functionality and performance of the GPS based navigation and timing system with the fully integrated spacecraft.

A. Signal Simulator Scenario

All HIL tests described in this section made use of Spirent signal simulators (STR7700 and STR4500) to generate artificial GPS signals representative of those received by an orbiting spacecraft. The modeled spacecraft is assumed to fly in a near circular, polar orbit at 728 km altitude. In accord with the envisaged "dusk-dawn" configuration, the ascending node is located at 6^h local time. The epoch is (fictitiously) chosen as 20 Dec. 2007, 12:00 GPS Time, and coincides with the ascending node crossing. Adopted orbital elements (in the inertial J2000 reference system) and the corresponding Earth-Centered-Earth-Fixed (ECEF) epoch state vector are given in Table 1. Within the inertial-to-ECEF transformation a UT1-TAI difference of –35.0 s and pole coordinates of $(x, y) = (0.0705", 0.4077")$ are applied by the simulator. The orbit is propagated over the 12.5 h simulation period using a JGM-3 70 x 70 Earth gravity model as well as drag perturbations. Ballistic properties of the satellite were modelled with assumed values of the cross-section A=0.5 m^2, the mass m=150 kg, and the drag coefficient C_D=2.3.

Table 1. Simulated PROBA-2 spacecraft orbit

Epoch	2007 Dec 20, 12:00:00 GPS; GPS week 1458, 388800s 2007 Dec 20, 11:59:46 UTC				
Elements (J2000)	Value	State vector (ECEF)		Value	
Semi-major axis (a)	7106.137 km	Position	x	6261.8006	m
Eccentricity (e)	0.000		y	-7106132.0234	m
Inclination (i)	98.302°		z	-5614.0912	m
Long. of ascend. node (Ω)	178.576°	Velocity	v_x	-1599.1846721	m/s
Arg. of perigee (ω)	0.0°		v_y	-7.2641697	m/s
Mean anomaly (M)	0.0°		v_z	7411.0611848	m/s

The GPS constellation is modeled based on the actual GPS almanac for week 1405, which is propagated to the scenario time within the signal simulator. The antenna diagram corresponds to a Sensor Systems S67-1575-141 antenna without ground plane as used on PROBA-2, which has earlier been calibrated in outdoor tests by DLR. To study the influence of key error sources, ionospheric path delays and broadcast ephemeris errors have been considered in most of the tests. The "spacecraft ionosphere model" (which implements the Lear mapping function[36]) and a constant total electron content (TEC) of $5 \cdot 10^{16}$ electrons/m^2 (=5 TECU) have been selected for the simulation of ionospheric effects. The impact of broadcast ephemeris and clock errors on the navigation solution has been modeled by considering constant offsets between the modeled GPS spacecraft position and the one described by the GPS navigation message. These offsets affect the simulated trajectory but are not included in the broadcast ephemeris message issued by the simulator. The offsets are constant in time and applied only to the radial satellite position. No tangential and normal offsets have been configured since this would not provide added realism to the simulation. In an effort to mimic a realistic Signal in Space Range Error (SISRE), the applied offsets are based on uniformly distributed random numbers with zero mean and a standard deviation of 1.5 m. For comparison, the performance of the current GPS constellation and ground segment achieves a representative SISRE of 1.0 to 1.5 m including both ephemeris and clock errors[37-38].

The orientation of the spacecraft in the PROBA-2 simulation scenario is designed to closely match the nominal attitude profile in Observation Mode. Here, the –x body axis is continuously oriented towards the Sun. The roll angle is chosen in such a way as to align the +z-, +y-, –z-, or – y-axis with the ecliptic north-pole, while maximizing the off-nadir angle of the star cameras. As an approximation of the true attitude, the initial orientation of the PROBA-2 spacecraft at the equator crossing is described by the heading, elevation and bank angles of 293°, 0°, and 180°, respectively, relative to the local North-East- Down frame. The orientation is held inertially fixed except for 90° roll rotations that are performed four times per orbit. These rotations are specified to take place at 14 min and 36

min after each equator crossing assuming an orbital period of 5960 s. Each rotation is completed within 3 mins. Even though the signal simulation cannot provide a fully rigorous replication of the PROBA-2 attitude profile, it is nevertheless considered sufficiently realistic to enable a proper pre-flight validation of the GPS navigation systems.

B. Phoenix-XNS Receiver Validation

The tracking and navigation performance of the Phoenix receiver was first validated in a series of standalone tests, in which the receiver was directly connected to the signal simulator via a low noise amplifier (LNA). Separate tests were conducted using the standard satellite selection (which assumes a zenith pointing antenna) and the PROBA-2 specific algorithm, which tries to replicate the actual attitude profile with its four roll rotations per orbit.

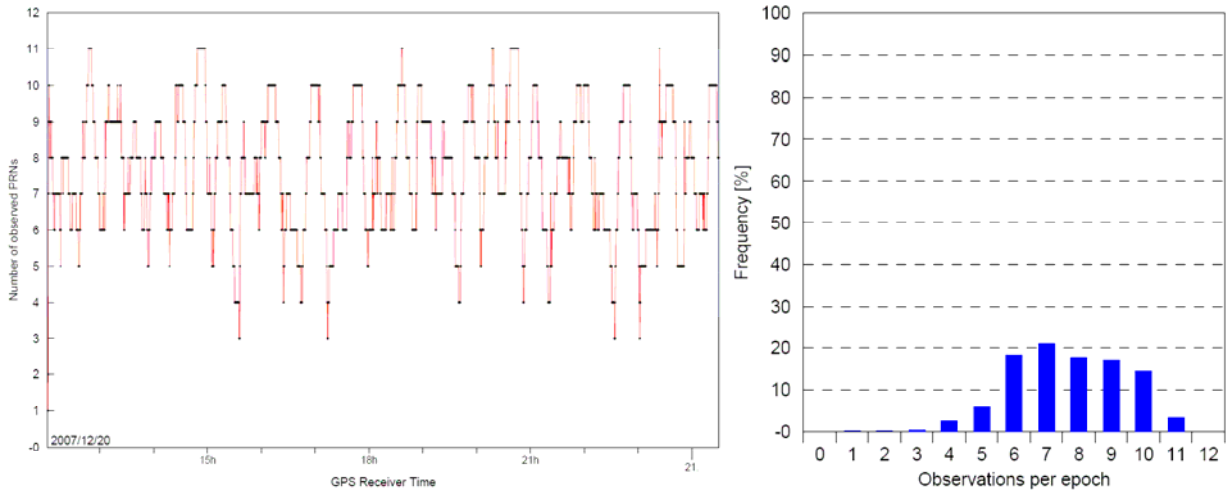

Figure 6. Timeline (*left*) and histogram (*right*) of the number of tracked GPS satellites using the default satellite selection algorithm

As illustrated in Fig. 6., it is well possible to track an adequate number of satellites for most of the time, even if the roll rotations are ignored in the prediction of visible satellites and the channel allocation. About 7-8 satellites can be tracked on average in this case. On the other hand, the kinematic navigation solution exhibits various gaps with typical durations of 5 min that coincide with attitude changes of the PROBA-2 spacecraft. Even though the number of tracked satellites rarely drops below the minimum of four, the position dilution of precision (PDOP) is strongly degraded in the respective cases and exceeds the adopted threshold (10) for an acceptable navigation fix.

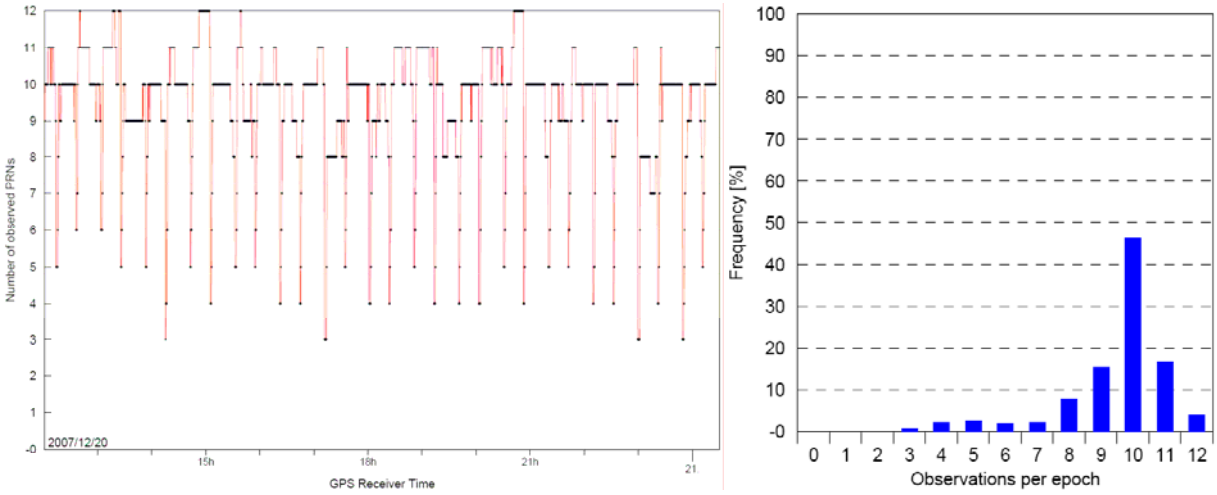

Figure 7. Timeline (*left*) and histogram (*right*) of the number of tracked GPS satellites using the PROBA-2 specific satellite selection algorithm

As expected, a notably larger number of GPS satellites can be tracked by considering the approximate attitude profile in the receiver (Fig. 7). On average, 10 satellites are received in this case and the probability of bad or missing navigation solutions is likewise reduced. Nevertheless, the number of tracked satellites is still drastically reduced in the vicinity of each roll maneuver, since the simplified Phoenix receiver model assumes an instantaneous change of the antenna boresight direction. As such, a temporary loss of the kinematic navigation solution cannot be ruled out in practice even with the refined model. With a maximum of 2 min, the outages are much shorter, however, than in the case of the default satellite selection. In any case, outages of several minutes are of no concern for the PROBA-2 operation and can always be bridged by the navigation filter (NAV function) of the ACNS onboard software.

Table 2. Phoenix real-time and offline positioning accuracy

Case	Description	Ephem. Errors	Iono. Errors	Channel Allocation	Radial [m]	Along-track [m]	Cross-track [m]	Position (3D rms)
I	Kinematic	none	none	Any	-0.04 ± 0.38	+0.23 ± 0.18	+0.01 ± 0.14	0.50 m
IIa	Kinematic	1.5m rms	5 TECU	Default	+3.19 ± 3.31	-0.51 ± 1.87	+0.07 ± 1.21	5.13 m
IIb				PROBA-2	+6.08 ± 3.18	-1.20 ± 2.06	-0.03 ± 1.38	7.38 m
IIIa	XNS (converged)	1.5m rms	5 TECU	Default	-0.04± 0.22	+0.07 ± 0.29	-0.07 ± 0.11	0.39 m
IIb				PROBA-2	+0.18 ± 0.33	-0.11 ± 0.47	-0.09 ± 0.11	0.63 m
IVa	Offline POD	n/a	5 TECU	Default	-0.03 ± 0.05	+0.19 ± 0.09	-0.06 ± 0.05	0.23 m
IVb				PROBA-2	-0.03 ± 0.03	+0.15 ± 0.07	-0.06 ± 0.06	0.19 m

The performance of the kinematic and filtered navigation solutions in the signal simulator tests is summarized in Table 2. Using realistic assumptions for the broadcast ephemeris errors and the total electron content (TEC), a representative 3D rms positioning accuracy of 5-7 m is achieved over the 12.5 h data arc with the purely kinematic solution (Case IIa/b). An obvious performance difference can be observed between the default channel allocation (Case IIa) and the PROBA-2 specific satellite selection (Case IIb). Even though a larger number of satellites is tracked in the latter case, an increased number of observations is performed at low elevations where they suffer from larger ionospheric effects and measurement noise. It may also be recognized that the kinematic position solution is shifted by an average of 3-5 m in radial direction with respect to the true orbit. This is a direct consequence of uncompensated ionospheric path delays in single frequency navigation solutions[36]. The actual offset depends on the distribution of tracked satellites and will vary in proportion to the TEC values encountered during the PROBA-2 mission.

The variation of the position errors for the kinematic navigation solution is illustrated in Fig. 8 for the default satellite selection mode. Due to the use of carrier phase smoothed pseudoranges, the kinematic positions exhibit a very small short term noise. On the other hand, the solution exhibits frequent steps, whenever the set of tracked satellites and the associated ionospheric and ephemeris errors change. The noise reduction achieved by the carrier phase smoothing is most obvious in an error-free simulation (Case I), in which case a representative 0.5 m accuracy is obtained.

The filtered XNS navigation solution (Cases IIIa/b) achieves an accuracy of better than 1 m after convergence to its steady state performance. At start-up, the XNS is initialized from the kinematic navigation solution and therefore exhibits a corresponding error of about 5 m with a predominant radial component. This initial error is removed within approximately 0.5-1 h, after which rms errors of 0.5 m or better are achieved in all axes. Evidently the XNS benefits from the ionosphere-free GRAPHIC measurements, but can also absorb part of the broadcast ephemeris errors in the estimation of the bias parameter. The variation of the XNS position errors after filter convergence is shown in Fig. 9 for the default satellite selection. As for the kinematic solution, somewhat inferior performance (0.6 m 3D rms steady state error) is again obtained when using the PROBA-2 specific satellite selection mode. Apparently, the XNS solution cannot fully benefit from the increased number of tracked satellites in this case, but suffers from the reduced accuracy of the initialization state vector.

For completeness we note that the GPS antenna offset of about 0.5 m from the center-of-mass cannot be properly considered during the PROBA-2 mission due to a lacking ACNS-to-GPS interface for instantaneous attitude information. As a result of the associated modeling uncertainty, a slightly reduced real-time navigation accuracy of about 1.5 m (3D rms) is expected in practice.

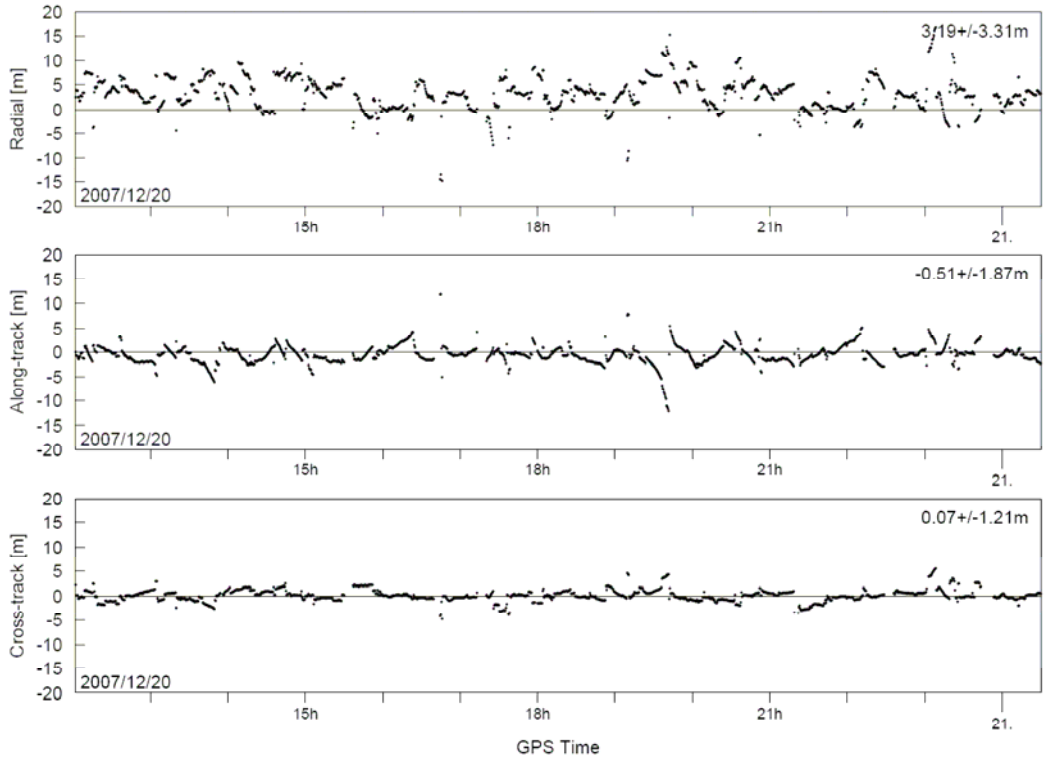

Figure 8. Position errors of the kinematic Phoenix navigation solution in the presence of broadcast ephemeris errors and ionospheric path delays (Case IIa)

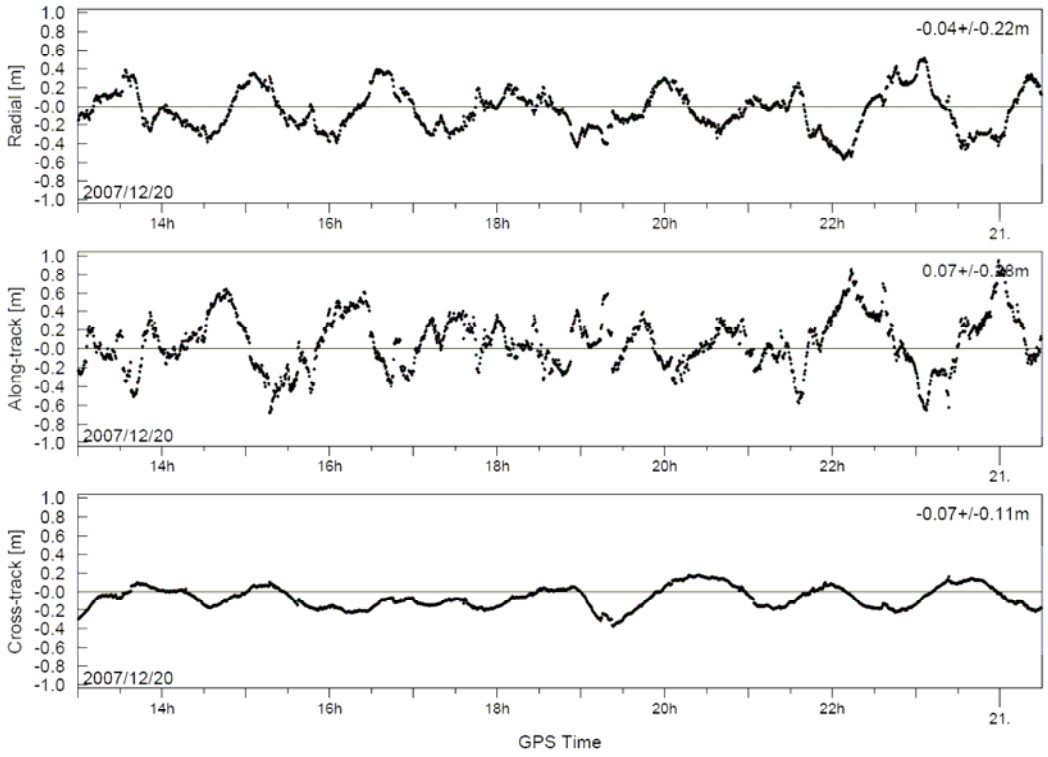

Figure 9. Position errors of the filtered Phoenix XNS navigation solution in the presence of broadcast ephemeris errors and ionospheric path delays (Case IIIa)

For further reference, the result of a precise orbit determination (POD) performed offline with the GHOST software[35] is given in Table 2 (Case IVa/b). The POD is based on 30 s samples of the raw pseudorange and measurements collected during the signal simulator test and involves the adjustment of the epoch state vector, a drag and radiation pressure coefficient, piecewise constant empirical acceleration at 10 min intervals, epoch wise clock offsets and, finally, pass-by-pass GRAPHIC biases. The GPS orbit and clock offsets are assumed to be known exactly, which is justified in view of the high quality (few cm) of the final GPS ephemeris products provided today by the International GNSS Service (IGS) and its analysis centers[39]. Likewise attitude information enabling an accurate modeling of the antennas offset is assumed to be known. The resulting accuracy of about 20 cm demonstrates the high navigation accuracy achievable even with single-frequency GPS and justifies the use of Phoenix based POD solutions as a reference for the flight validation of the PROBA-2 real-time navigation components. No relevant dependence of the POD performance on the channel allocation algorithm and the resulting number and distribution of tracked satellites can be deduced from the respective test results of Cases IVa and IVb. Finally, it may be noted that the POD process enables an estimation of continuous thrust maneuvers along with the other adjustment parameters. Subject to the availability of raw GPS measurements in the respective operations phase it can thus contribute to a proper calibration of the SSTL propulsion system, which constitutes one of the innovative PROBA-2 technology experiments.

Table 3. Phoenix real-time and offline velocity solution accuracy

Case	Description	Ephem. Errors	Iono. Errors	Channel Allocation	Radial [m/s]	Along-track [m/s]	Cross-track [m/s]	Velocity (3D rms)
I	Kinematic	none	none	Any	+0.001 ± 0.051	+0.000 ± 0.023	+0.000 ± 0.018	0.059 m/s
IIa	Kinematic	1.5m rms	5 TECU	Default	-0.003 ± 0.053	-0.004 ± 0.023	+0.000 ± 0.018	0.061 m/s
IIb				PROBA-2	+0.005 ± 0.041	-0.007 ± 0.024	+0.000 ± 0.018	0.051 m/s
IIIa	XNS (converged)	1.5m rms	5 TECU	Default	-0.0002±0.0003	+0.0000±0.0002	+0.0000±0.0002	0.0005 m/s
IIb				PROBA-2	+0.0001±0.0006	-0.0001±0.0003	+0.0000±0.0002	0.0007 m/s
IVa	Offline POD	none	5 TECU	Default	-0.0002±0.0001	-0.0000±0.0001	-0.0000±0.0001	0.0002 m/s
IVb				PROBA-2	-0.0002±0.0001	-0.0000±0.0000	-0.0000±0.0001	0.0002 m/s

A summary of the real-time and offline velocity accuracy is given in Table 3. In case of the kinematic solution a 3D rms accuracy of about 5 cm/s is achieved, which reflects the noise level (1-2 cm/s) of the carrier phase-based range-rate measurements in the Phoenix receiver. In comparison with this, an improvement by up to two orders of magnitude is achieved with the dynamically filtered XNS solution. As a result, the semi-major axis of the orbit is known with high reliability which enables accurate orbit predictions based on the estimated state vector. In fact, the XNS is able to propagate the PROBA-2 orbit with an accuracy of better than 10 m for more than two revolutions in case of a loss of GPS tracking. This is particularly noteworthy since the dynamical models employed in the simulator are intentionally different from the XNS navigation filter to reflect the limited knowledge of the real-world dynamics in the onboard application. For illustration, Fig. 10 shows the evolution of the XNS along-track position error relative to the simulator truth orbit for 3 h past the end of available GPS measurements.

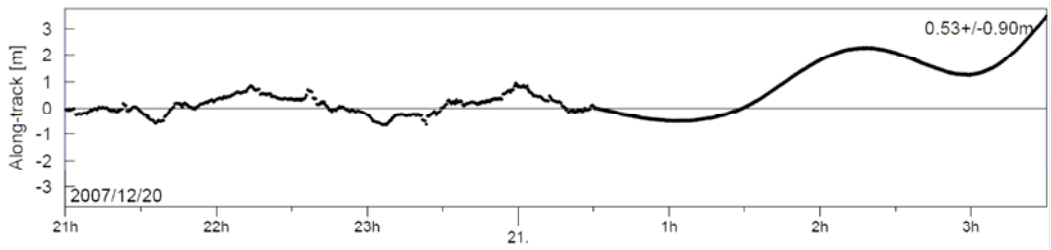

Figure 10. Along-track position error of the filtered Phoenix XNS navigation solution beyond the end of the GPS tracking arc on June 21, 0^h30^m (Case IIIa)

C. Integrated GPS/ACNS System Test

Complementary to the stand-alone tests of the Phoenix GPS receiver and the XNS navigation system, an integrated system test was conducted in January 2008 to validate the proper interaction of the receiver with the onboard computer and the ACNS software. For this purpose, a portable GPS signal simulator was installed in the integration hall at Verhaert and simulated GPS radio-frequency (r/f) signals were transmitted to the PROBA-2 spacecraft via a re-radiation kit (Fig. 11). All relevant flight units (GPS, ADPMS, etc.) were installed in the spacecraft bus, which could be operated via an umbilical and the electrical ground support equipment (EGSE). Parallel to the GPS navigation chain, the full ACNS system was operated during the integrated GPS/ACNS test. Where required, stimuli from the PROBA-2 Software Verification Facility (SVF) were used to represent flight hardware components that could not be operated under realistic conditions. For use within the onboard orbit propagator of the ACNS software, NORAD type twoline orbital elements were generated and uploaded to the spacecraft, which approximate the simulated orbit with an accuracy of about 200 m over a 12.5 h interval.

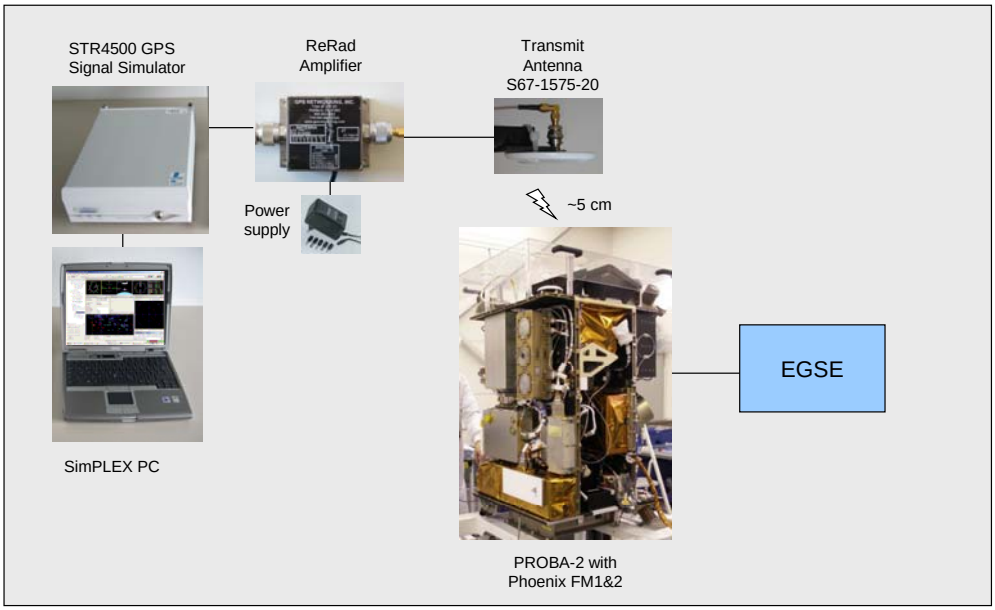

Figure 11. Test setup for integrated HIL testing of the PROBA-2 GPS and ACNS system

The scenario used to generate the artificial GPS signals matched the one employed in the stand-alone receiver tests described above and included both broadcast ephemeris errors and ionospheric path delays. However, the focus of the integrated system test was less on performance aspects than on the proper interaction and robustness of the various system components. As such the receiver was not provided with time, orbit , and almanac information after power-up, but performed only cold-starts. Likewise, the default firmware settings of the Phoenix receiver were used throughout and no commands were given to select the PROBA-2 antenna pointing or to upload the proper Earth-orientation parameters for the XNS operations. For the overall system validation the following activities were conducted in the integrated test:

- Two consecutive cold starts were performed, after which the receiver required 22 min and 16 min, respectively, to achieve a first valid navigation solution. The first of these cold starts coincided with a simulated 90° slew, which explains the slightly larger acquisition time. While the PROBA-2 specific cold start time-to-first fix is certainly larger than for spacecraft with a permanently zenith facing antenna, it is generally acceptable for the mission. If necessary, dedicated procedures are available in the Redu mission operations center to perform an aided warm start of the receiver.
- An intentional loss of navigation was enforced by raising the receiver elevation mask from 5° to 60° and thus restricting the number of tracked satellites below a minimum of four for a period of about five minutes. During this time, the NAV function of the ACNS software continued to provide propagated orbit information.
- An extended loss of navigation was enforced for more than 25 min. The Fault Detection Isolation and Recovery (FDIR) mechanisms properly recognized this condition and performed a switch to the

redundant Phoenix GPS unit. During the initial signal acquisition phase of this receiver, orbit information for the ACNS was generated based on the twoline elements.

- An extended loss of navigation was enforced on the redundant receiver. After 25 min the twoline elements orbit propagator was automatically used to provide orbit information of the attitude control system.

These test steps validated the proper handling of GPS related anomalies by the onboard FDIR function. In addition, the proper function of the ACNS timing function (TIM) could be validated, which synchronized the various onboard clocks (processor, star camera, etc.) with GPS and UTC time.

Over the three hours test data arc the kinematic navigation solution of the Phoenix receiver exhibits a 3D rms position error of 5.5 m and peak errors of 12.5 m. While this is in close accord with the results obtained previously in the long-duration stand alone receiver tests (cf. Table, Case IIa), the same does not apply for the XNS solution. Due to the lack of proper Earth orientation parameters, a notable (1 m rms) cross-track error shows up in the XNS result. Overall, a position 3D rms position error of 1.8 m is obtained, which includes the start-up phase of about 30 min. For illustration, the evolution of the radial position error over the 3 h test data arc is shown in Fig. 12 for both the kinematic and filtered solution. The onboard navigation filter achieved an rms position accuracy of better than 10 m over the same data arc, which is well within the system specification and demonstrated its proper function and implementation[6].

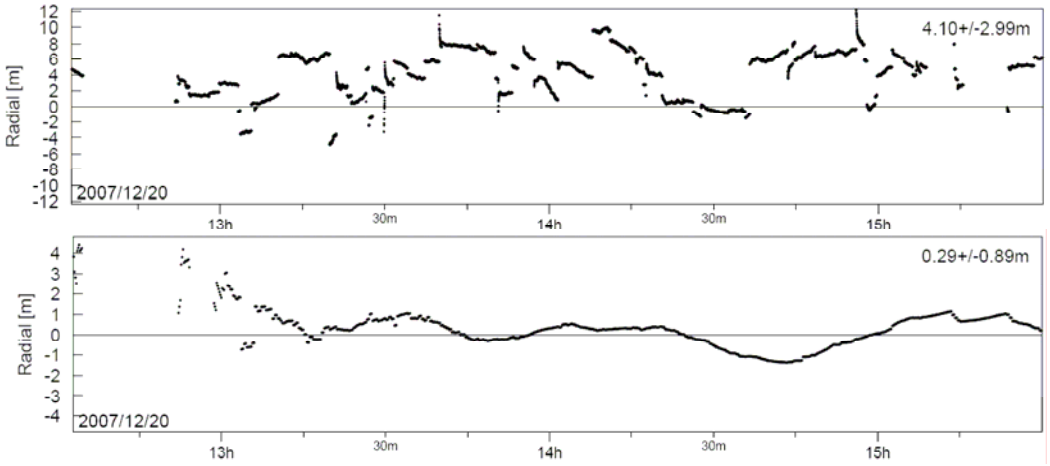

Figure 12. Radial position error of the kinematic and filtered Phoenix navigation solution during the integrated system test

VI. Conclusion

The PROBA-2 spacecraft is equipped with a unique complement of GPS navigation sensors and real-time navigation systems that are designed to deliver onboard position information with a 1-10 m accuracy. A concise performance characterization of each of these components will be supported by a laser retro reflector which is otherwise only found on geodetic science missions. Aside from the in-flight validation of individual hard- and software components, the PROBA-2 technology demonstration mission thus offers a highly attractive testbed for the evaluation and comparison of GPS based autonomous navigation systems. The wide range of different technologies hosted by the PROBA-2 spacecraft will contribute to a better trade-off between single- and dual-frequency GPS, between commercial-off-the-shelf and space-grade sensor technology, and, finally, between accuracy and complexity of navigation systems. It will thus provide system designers with valuable information for the assessment and selection of navigation technology in future LEO missions.

The preflight validation of the PROBA-2 navigation system components has greatly benefited from hardware-in-the-loop simulations conducted in a signal simulator test bed. These have enabled a realistic performance assessment and demonstrated the proper interaction of relevant hardware and software elements in a real-time environment. The use of HIL simulations is strongly recommended for all missions considering GPS sensors as primary navigation and timing sensor for onboard usage.

The Phoenix XNS navigation system has demonstrated an excellent performance in the signal simulator tests. Real-time positioning accuracies of down to 0.5 m (3D rms) and a velocity estimation to the level of 0.5 mm/s (3D rms) have been achieved during continuous GPS tracking. Based on this, the orbit could be propagated with a 10m level accuracy over period of 3 h. The tests provide good evidence that even single-frequency can meet advanced real-time navigation requirements of future remote sensing missions.

Acknowledgments

Satellite laser ranging of the PROBA-2 spacecraft for validating the precise orbit determination and navigations functions will be provided by the International Satellite Laser Ranging Service (ILRS) using its world-wide net of SLR tracking stations. Their envisaged support is gratefully acknowledged.

References

[1]Teston F., Creasey R., Bermyn J., Mellab K., "PROBA: ESA's Autonomy and Technology Demonstration Mission", Paper IAA-97-11.3.05, *Proceedings of the 48th International Astronautical Congress*, 1997

[2]Gantois, K., Teston, F., Montenbruck, O., Vuilleumier, P., van den Braembussche, Markgraf, M., "PROBA-2 Mission and New Technologies Overview", *Small Satellite Systems and Services - The 4S Symposium*; 25-29 September 2006; Chia Laguna Sardinia, Italy, 2006

[3]de Lafontaine, J., Buijs, J., Vuilleumier, P., van den Braembussche, P., Mellab, K., "Development of the PROBA Attitude Control and Navigation Software", *Proceedings of the 4th ESA International Conference Spacecraft Guidance, Navigation and Control System*s, held 18-21 October, 1999 in ESTEC, Noordwijk, the Netherlands. Edited by B. Schürmann. ESA SP-425. Paris: European Space Agency, 2000., p.427

[4]Gill E., Montenbruck O., Kayal H.; "The BIRD Satellite Mission as a Milestone Towards GPS-based Autonomous Navigation"; *Navigation - Journal of the Institute of Navigation* 48/2, 69-75, 2001

[5]de Lafontaine, J., Côté, J., Kron, A., Vuilleumier, P., Santandrea, S., van den Braembussche, P., "Validation of Innovative State Estimation and Control Techniques on Proba-2", 6th *ESA Conference on Guidance, Navigation and Control Systems*, Loutraki, Greece, 2005

[6]de Lafontaine, J., Côté, J., Kron, A., Naudet, J., Van den Braembussche, P., "PROBA-2: AOCS Software Validation Process and Critical Results", *7th ESA Conference on Guidance, Navigation and Control Systems*, 2-5 June 2008,Tralee, Ireland, 2008

[7]Serre, S., Mehlen, Ch., Boyer, C., Holsters, P., Seco-Granados, G., Garcia-Rodriguez, A., Issler, J.-L., Grondin, M.; "A Dual Frequency GPS Receiver (L1/L2c or L1/Lp) for Space Applications in LEO and GEO Orbit"; *ION-GNSS-2006*, September 26-29, 2006, Fort Worth, Texas, 2006

[8]IS-GPS-200D,"Interface Specificaton: Navstar GPS Space Segment/Navigation User Interfaces", Navstar GPS Joint Program Office, September 2004. Available online at http://www.navcen.uscg.gov/gps/geninfo/IS-GPS-200D.pdf

[9]Rizos, Ch., "The Future of Global Navigation Satellite Systems", 3rd Workshop for Space, Aeronautical & Navigational Electronics, Perth, Australia, 15-18 April, Procs in IEICE Tech. Rept. 107(2), 25-30, 2007

[10]Pearlman, M.R., Degnan, J.J., and Bosworth, J.M., "The International Laser Ranging Service", *Advances in Space Research*, Vol. 30, No. 2, pp. 135-143, July 2002, DOI:10.1016/S0273-1177(02)00277-6

[11]Montenbruck, O., Nortier, B., Mostert, S., "A Miniature GPS Receiver for Precise Orbit Determination of the SUNSAT2004 Micro-Satellite"; *ION National Technical Meeting*, 26-28 Jan. 2004, San Diego, California, 2004

[12]Ebinuma T., Unwin M., Underwood C., Imre E.; "A Miniaturized GPS Receiver for Space Applications"; *16th IFAC Symposium on Automatic Control in Aerospace*; 14-18 June 2004, St. Petersburg, Russia, 2004

[13]Markgraf M., Montenbruck O., Metzger S.; "Radiation Testing of Commercial-off-the-Shelf GPS Technology for use on LEO Satellites"; *2nd ESA Workshop on Satellite Navigation User Equipment Technologies, NAVITEC'2004*, 8-10 Dec. 2004, Noordwijk, The Netherlands (2004).

[14]Unwin, M., Underwood, C., Frydland, A., Jameson, P., Harboe Sorensen, R.; "A New Miniaturised GPS Receiver for Space Applications", *ION-GPS-2004*, Portland, Oregon, 2004

[15]Montenbruck, O., Gill, E., Markgraf, M., "Phoenix-XNS - A Miniature Real-Time Navigation System for LEO Satellites"; *3rd ESA Workshop on Satellite Navigation User Equipment Technologies*, *NAVITEC'2006*, 11-13 December 2006, Noordwijk 2006

[16]Potti, J., Carmona, J.C., Bernedo, P., Silvestrin, P., "An autonomous GNSS-based orbit determination system for low-Earth observation satellites", *Proc. ION GPS-95*, Institute of Navigation, 12-15 Sept 1995, Palm Springs, CA, pp 173-182, 1995

[17]Hart, R.C, Hartman, K.R., Long, A.C., Lee, T., Oza, D.H. "Global Positioning System (GPS) Enhanced Orbit Determination Experiment (GEODE) on the Small Satellite Technology Initiative (SSTI) Lewis Spacecraft", *Proc. ION GPS 96*, 1996

[18]Goldstein, D.B., Born, G.H., Axelrad, P. "Real-Time, Autonomous, Precise Orbit Determination Using GPS", Navigation 48(3):155-168, 2001

[19]Vallado, D. A.; *Fundamentals of Astrodynamics and Applications*; 2nd ed.; Space Technology Library, Kluwer Academic Publishers; Dordrecht (2001).

[20]Montenbruck, O., Gill, E.; *Satellite Orbits*; Springer Verlag, Heidelberg (2000).

[21]Tapley B. D., Schutz B. E., Born G.; *Statistical Orbit Determination*; Elsevier Academic Press (2004).

[22]UT/CSR; "GRACE Gravity Model GGM01"; Center for Space Research, University of Texas; Austin, 2003. URL http://www.csr.utexas.edu/grace/gravity/ggm01/GGM01_Notes.pdf; last accessed Oct. 2004.
[23]Cunningham, L. E.; "On the Computation of the Spherical Harmonic Terms needed during the Numerical Integration of the Orbital Motion of an Artificial Satellite"; *Celestial Mechanics* 2, 207–216, 1970
[24]Montenbruck, O., Ramos-Bosch, P.; "Precision Real-Time Navigation of LEO Satellites using Global Positioning System Measurements"; *GPS Solutions* 12/3,187-198, 2008. DOI 10.1007/s10291-007-0080-x
[25]Rizos, C., Stolz, A.; "Force Modeling for GPS Satellite Orbits"; *1st Int. Symposium on Precise Positioning with GPS*, Vol. 1, pp. 87-98, Rochville, USA, 1985.
[26]Harris, I., Priester, W.; "Time-Dependent Structure of the Upper Atmosphere"; *NASA TN D-1443*; Goddard Space Flight Center, Maryland, 1962.
[27]McCarthy, D. D.; "IERS Conventions (1996)"; IERS Technical Note 21; Central Bureau of IERS - Observatoire de Paris; Paris, 1996.
[28]Seidelmann, P. K. (ed.); *Explanatory Supplement to the Astronomical Almanac*; University Science Books, Mill Valley, California, 1992.
[29]Hairer, E., Norsett, S. P., Wanner, G.; *Solving Ordinary Differential Equations I*; Springer-Verlag, Berlin-Heidelberg-New York, 1987
[30]Montenbruck, O., Gill, E.; "State Interpolation for On-board Navigation Systems"; *Aerospace Science and Technology* 5, 209-220 (2001). DOI 10.1016/S1270-9638(01)01096-3
[31]Yunck T.P.; "Orbit Determination"; in: Parkinson B.W., Spilker J.J. (eds.); *Global Positioning System: Theory and Applications*. AIAA Publications, Washington DC, 1996
[32]Misra, P., Enge, P.; *Global Positioning System (GPS): Signals, Measurements & Performance;* Ganga-Jamuna Press, 2nd ed. 2006
[33]Gill, E., Montenbruck, O.; "Comparison of GPS-based Orbit Determination Strategies"; *18th International Symposium on Space Flight Dynamics*, 11-15 Oct. 2004, Munich, Germany, 2004
[34]Schmidt, R., Baustert, G., König, R., Meixner, H., Neumayer, K.-H., Reigber, Ch.; „The Development of Automated Processing of Orbit Predictions for CHAMP", in: *Proceedings of the International Workshop on Laser Ranging*, November 2000, Matera, Italy, 2000
[35]Montenbruck, O., van Helleputte, T., Kroes, R., Gill, E.; "Reduced Dynamic Orbit Determination using GPS Code and Phase Measurements"; *Aerospace Science and Technology* 9/3; 261-271, 2005
[36]Garcia-Fernandez M., Montenbruck O.; "Low Earth orbit satellite navigation errors and vertical total electron content in single-frequency GPS tracking"; Radio Science 41, RS5001 (2006). DOI 10.1029/2005RS003420
[37]Warren, D.L.M., Raquet, J.F., "Broadcast vs precise GPS ephemerides: a historical perspective", *GPS Solutions* 7, 151–156, 2003
[38]Creel, T., Dorsey, A. J., Mendickim P.J., Little, J., Mach, R.G., Renfro, B. A., "The Legacy Accuracy Improvement Initiative", *GPS World* 17/3, 20, 2006
[39]Dow J.M., Neilan R.E., Gendt G., "The International GPS Service (IGS): Celebrating the 10th Anniversary and Looking to the Next Decade," Adv. Space Res. 36 vol. 36, no. 3, pp. 320-326, 2005. doi:10.1016/j.asr.2005.05.125